Extracellular traps in skin lesions infected with lymphocystis disease virus in black rockfish (*Sebastes schlegelii*)

Qian Li | Heng Chi | Xianghu Meng | Roy Ambli Dalmo |Xiuzhen Sheng | Xiaoqian Tang | Jing Xing | Wenbin Zhan

[1] Laboratory of Pathology and Immunology of Aquatic Animals, KLMME, Ocean University of China, Qingdao 266003, China

[2] Laboratory for Marine Fisheries Science and Food Production Processes, Qingdao National Laboratory for Marine Science and Technology, Qingdao, China

Correspondence

Heng Chi, Laboratory of Pathology and Immunology of Aquatic Animals, Fisheries College, Ocean University of China, Qingdao 266003, China

Email: chiheng@ouc.edu.cn

Funding information

This research was funded by grants from the National Key Research and Development Program of China (2023YFD2400703), the Fundamental Research Funds for the Central Universities (No. 202212012), the National Natural Science Foundation of China (32373160 & 31872594), and the Young Talent Program of Ocean University of China (No. 2022010042). The Research Council of Norway (grant no. 301401 and 32519) is also acknowledged.

Abstract:

The lymphocystis disease (LCD), caused by Lymphocystis disease virus (LCDV), is a benign and self-limiting disease described in a many freshwater and marine fish species. Hypertrophic fibroblasts and extensive aggregation of inflammatory cells are characteristics of LCD. In the present study, small animal imaging and ultrastructural investigations were carried out on the lymphocystis nodules of black rockfish (*Sebastes schlegelii*) naturally infected with lymphocystis iridovirus, to assess pathology, and the exudate with particular attention to the formation of extracellular traps (ETs) *in vivo*. Ex *vivo* were examined by nodules sections and primary cells stimulation. By histopathological analysis, the nodules contained infiltrated inflammatory cells and extensive basophilic fibrillar filaments at the periphery of the hypertrophied fibroblasts. ETs were assessed in nodules samples using indirect immunofluorescence to detect DNA and histones. Moreover, LCDV was able to infect peritoneal cells of black rockfish *in vitro* and induce the formation of ETs within 4 hours. In summary, this study proved that ETs are involved in the response to LCDV infection and may be involved in formation of lymphoid nodules. Taken together, the findings provide a new perspective to determine the impact factors on the growth of nodules.

Keywords: Lymphocystis disease virus; Extracellular traps; Lymphocystis nodules; Fish

1 | INTRODUCTION

Black rockfish (*Sebastes schlegelii*) is widely distributed in Japan, Korea, and northeast of China (Kim et al., 2001), and is of economic importance. The Black rockfish is susceptible to lymphocystis disease virus (LCDV), causing lymphocystis disease (LCD). LCDV is a member of iridoviridae family and infects at least 140 different marine and freshwater fish species worldwide (Anders, 1989). LCDV primarily affects dermal fibroblasts, causing papilloma-like hypertrophy or nodular masses (Samalecos, 1986). Nodules may be solitary or clustered, either on the skin or in the internal organs. Infected host cells are called lymphocystis cells or lymphocysts (González de Canales et al., 1996; Paperna et al., 1982). Lymphocystis disease is usually self-limiting (resolves spontaneously), where the host usually are recovering within a few weeks after the lesions have resolved (Paperna et al., 1982; Roberts, 1976). However, secondary infection such as by bacterial or by water mold may be fatal to fish. The economic loss is due to the their unsightly appearance which lower human perception of fish with lesions.

Neutrophils are terminally differentiated leukocytes that have evolved to protect the animal host upon inducing potent antimicrobial responses against invading pathogens. During activation, neutrophils become efficient killers, utilizing toxic intracellular granules (Flerova & Balabanova, 2013; Meseguer et al., 1994), reactive oxygen species (ROS) (Katzenback & Belosevic, 2009; Rieger et al., 2012; Wilhelm Filho, 2007), and deploying neutrophil extracellular traps (NETs) (Palić et al., 2007; Pijanowski et al., 2013) to arrest and/or kill microorganisms. NETs are composed of chromatin fibers,

64 DNA coated with granule proteins such as histones, enzymes (e.g. myeloperoxidase or
65 elastase) and antimicrobial peptides (e.g. cathelicidins) (Papayannopoulos et al., 2010;
66 Urban et al., 2009). Eosinophils and mast cells also produce DNA containing NET-like
67 extracellular traps (ETs) in response to pathogens or proinflammatory stimuli (Gómez
68 et al., 2021). Currently, *in vivo* and in vitro experiments have confirmed that ETs can
69 capture extracellular microbes such as bacteria, parasites, and fungi, and their formation
70 has also been observed in the context of viral disease, including influenza, HIV-1, hanta
71 and poxvirus infection (Brinkmann et al., 2004; Jenne et al., 2013; Jenne & Kubes,
72 2015; Narasaraju et al., 2011; Raftery et al., 2014a; Saitoh et al., 2012). ETs may kill
73 the pathogens through various antibacterial proteins after capture and may also aid other
74 immune cells to phagocytose and degrade foreign microorganisms. Furthermore,
75 excessive ETs formation has also been observed in several pathological cases. For
76 example, endogenous crystals (cholesterol or monosodium urate crystals) can induce
77 PAD4-dependent ETs that promotes inflammatory diseases such as atherosclerosis,
78 gout, and pancreatitis (Warnatsch et al., 2015; Desai et al., 2016; Schauer et al., 2014).
79 In a tumor-free environment, ETs formation also serve as physical scaffolds in the
80 metastatic niche, and deposited ETs can efficiently trap circulating cancer cells
81 facilitating their adhesion to the tissue stroma (Najmeh et al., 2017).

82 Recently, the presence of ETs has been documented in a variety of fish species,
83 including tongue sole, turbot, carp, and Atlantic salmon, and have been attributed to be
84 involved in response to bacterial infection (Álvarez de Haro et al., 2021; Chi & Sun,
85 2016; Pijanowski et al., 2013; Wen et al., 2018). However, no information exists about

the presence of ETs in skin nodules from fish that suffer from lymphocystis disease. Thus, the present study is aimed to investigate whether ETs are produced in lymphoid nodules, and assess whether rockfish cells infected with LCDV produce ETs during *in vivo* and *ex vivo*.

2 | MATERIALS AND METHODS

2.1 | Fish, Virus and Antibodies

Healthy black rockfish (*Sebastes schlegelii*), 28-30 cm, were obtained from a fish farm in Rizhao city of Shandong province, China. Fish were confirmed as LCDV-free via PCR (Zhan et al., 2010), and acclimated in aerated seawater at 22 ºC for one week and fed daily with dry food pellets before use. The diseased black rockfish infected by lymphocystis disease virus were obtained from another fish farm. The protocols for animal care and handling used in this study were approved by the Animal Care and Use Committee of Ocean University of China (Permit Number: 20180101). All possible efforts were dedicated to minimizing suffering.

The GenBank accession number of the LCDV-HD virus strain genome sequence used in this study was DQ279090. Source of virus? The final concentration of virus was adjusted to 1 mg in 1 mL (is this right?) sterile phosphate buffered saline (PBS, pH 7.4), and the 50% tissue culture infective dose ($TCID_{50}$) was determined using Reed-Muench method (Zhong et al., 2018). Rabbit anti-LCDV polyclonal antibody, previously produced in our laboratory was used in this experiment (Wang et al., 2011).

2.2 | Visualization of extracellular traps ex vivo on the surface of lymphocystis nodules

To obtain ex vivo explants, nodules were cut off along with the skin or fins and placed in glass dishes. The nodules were subsequently immersed in a SYTOX™ Green bath (80 mg ml^{-1}) for ten minutes to stain extracellular DNA. After gentle washing three times with PBS, extracellular DNA was assessed using a fluorescence stereomicroscope (Leica Microsystems, Berlin, Germany) and small animal imaging instruments (Vilber Bio Imaging Fusion FX6, Collegien, France) using excitation and emission wavelengths of 488 and 523 nm, respectively.

2.3 | Collection of epidermal mucus from skin areas with nodules and scanning electron microscopy

Mucus was carefully scraped off from the surface of the nodules using a soft rubber spatula. Care was taken to avoid cell ruptures. Mucus samples were thoroughly mixed with equal quantity of sterilized PBS and settled on a round cover glass in a cell culture well and fixed with 2.5% glutaraldehyde (Hushi, Shanghai, China) for 2 h. The samples were dehydrated in a series of increased concentration of ethanol (30, 50, 70, 80, 90 and 100%) for 10 minutes at room temperature in each step, then treated with isoamyl acetate for 10 minutes, critical point-dried (Hitachi-HCP, Hitachi, Tokyo, Japan), sputter-coated with platinum (MC1000, Hitachi, Tokyo, Japan) and examined by a scanning electron microscopy (SEM) (S-3400N, Hitachi, Tokyo, Japan).

2.4 | Preparation of specimens for histology/histopathology

The dissected nodules were washed with TNE buffer (50 mM Tris, 100 mM NaCl, 1 mM EDTA, pH 7.4) and fixed in Bouin's fixative for 24 hours, and then washed three times with 70% ethanol. The nodules were dehydrated in a graded series of ethanol and

cleared in xylene. Subsequently, the samples were embedded in paraffin by using standard procedures to make 5 μm-thick sections from transversal and sagittal orientations. The sections were stained with hematoxylin and eosin (HE) for histological observation by Zeiss microscope (Zeiss, Jena, Germany). For preparing cryostat sections, the dissected nodules were immersed in a tissue-freezing medium (OCT, Jung, USA) and immediately and frozen at -80 ºC. Thereafter, sections at 5 μm thickness were obtained using freezing microtome (Leica, Berlin, Germany). The aceton-immersed sections were placed onto a glass slide and dried in a fume cupboard for 10 min, before the immunofluorescence assay.

2.5 | Immunodetection of ETs

The cryostat sections were firstly blocked with 5% bovine serum albumin (BSA) for 60 minutes, then incubated for 1 hour with 1:500 mouse anti-histone 3 (H3) monoclonal antibody (EASYBIO, Beijing, China) at RT. After washing three times with PBS, the sections were incubated for 1 hour with 1:1000 rabbit anti-mouse IgG antibody labeled by Alexa Fluor 649 (Sigma St. Louis, MO, USA). DNA was stained by 4′,6-diamidino-2-phenylindole (DAPI, Bio-Legend, Santiago, Chile) for 5 minutes. After DAPI staining, the sections were analyzed using a fluorescence microscopy (Zeiss, Jena, Germany).

2.6 | LCDV infection *in vitro* and indirect immunofluorescence assay

To obtain intraperitoneal cells, black rockfish were intraperitoneally injected with 30 ml L-15 medium, the abdomen was gently massaged to get peritoneal cells exuded. Peritoneal fluid was withdrawn by a syringe and thereafter centrifuged at 500 *g* for 10

minutes. The cell pellets were resuspended in 5 ml L-15 medium and washed again by centrifugation at 480 *g* for 5 minutes.

Since ETs are fragile, each step was done with maximal care to preserve the fibrous nanostructures. Peritoneal cells were seeded onto round glass coverslips (12 mm) that previously had been treated with 0.001% poly-L-lysine (Sigma, St. Louis, MO, USA), in 24-well cell culture plates (Corning Costar, Cambridge, MA, USA) at 1×10^6 cells $well^{-1}$ concentration. After the cells attached, the peritoneal cells were stimulated (infected) with 4 $TCID_{50}$ ml^{-1} LCDV at 22 ºC for 3 hours. Non-stimulated cells were served as controls. After removing free virus particles by three times PBS washes, the peritoneal cells were fixed by 4% paraformaldehyde (Sigma Biotech, Shanghai, China) for 20 min at room temperature. After removing the paraformaldehyde by washing of coverslips, any non-specific binding sites of the specimens were blocked with 5% BSA for 60 minutes. Subsequently, the cells were incubated with rabbit anti-LCDV antibody (1:1000) as primary antibody for 1 hour at 37 ºC. After three washes with PBS, the coverslips were incubated with fluorescein isothiocyanate FITC-conjugated goat anti-rabbit Ig antibody (1:1000, Sigma, USA) for 1 hour at 37 ºC in the dark. DAPI (Roche, Basel, Switzerland) staining was used to visualize the cell nuclei. The coverslips were observed under a fluorescence microscopy (Zeiss, Jena, Germany).

2.7 | Fluorometric assay for the quantification of ETs *in vitro*

The quantification of ETs was performed as reported previously (Parker et al., 2012). Briefly, peritoneal cells (5×10^6 cells ml^{-1}) were suspended in phenol red-free L-15 medium and seeded in a black 96-well plate (200 µl $well^{-1}$) (Cayman Chemical, Ann

Arbor, MI, USA). The cells were treated with PMA (100 ng mL^{-1}) and infected with 4x $TCID_{50}$ ml^{-1} LCDV for 0, 1, 2, or 4 hours. Time-matched control cells were not stimulated or infected. The PMA-stimulated group were used as a positive control and the PBS-treated cells were served as negative control. Fluorescence was then quantified as relative fluorescence units (RFU) at 485 nm excitation and 530 nm emission using a fluorescence spectrophotometer (POLARstar OPTIMA, Ortenberg, Germany).

2.8 | Statistical analysis

All experiments were performed more than three times, and statistical analyses were performed by using the one-way ANOVA followed by LSD multiple group comparisons in the SPSS 18.0 software (SPSS Inc., Chicago, IL, USA). Data were expressed as mean ± standard deviation, and statistical significance was defined as $P < 0.05$.

3 | RESULTS

3.1 | Characterization lymphocystis nodules

Black rockfish suffering lymphocytosis showed multifocal, diffuse, gray pink, round, firm, papilloma / tumor like nodules on the skin of the body and fins, with some nodules covering epithelial tissue rich in chromatophores. The color of the chromatophores was grey to reddish. The diameter size of the skin nodules ranged from 0.2 to 2 cm (Figure 1a). Histopathologic examination of sections obtained from the fin and skin nodules revealed hypertrophic lymphocystis cells with varied size (100-300 µm) (Figure 1b-c). Cropped micrograph of lymphocystis cells showed an irregular or disappeared nucleus and thick smooth hyaline capsules. Many inclusion bodies, which

were strongly stained by hematoxylin and eosin (H&E), were observed peripherally near the membrane of the hyaline capsule. Infiltration of inflammatory cells between hypertrophic cells were observed. A high number of the inflammatory cells exhibited the typical nuclear characteristics of ET-producing cells including a lobulated nuclei and abundance of basophilic fibrillar filaments (Figure 1c).

3.2 | Exudated ETs on the surface of lymphocystis nodules from diseased fish - *ex vivo* study

We investigated any presence of surface-associated DNA of lymphocystis nodules from black rockfish by in-situ staining with a membrane-impermeable DNA dye (Sytox™ Green) followed by fluorescence microscopy. All the nodules showed filiform structures of extracellular DNA on the surfaces (Figure 2a-c). In addition, intense fluorescent signals from Sytox™ Green labelling of the surface of the nodules were confirmed by small animal imaging. The large nodules showed stronger fluorescence intensity than smaller ones (Figure 2d-e). The analysis of the quantitative region of interest (ROI) showed that the fluorescence intensity in the large nodules were 3.3-fold higher than in the small nodules. To identify the morphology of ETs in the mucus on the surface from the nodules, the ultrastructural studies using SEM revealed presence of individual fiber and bundles of chromatin fibers - coalesced into netlike structures. These were localized between different cells (Figure 2f).

3.3 | Lymphocystis nodules contain abundant extracellular DNA

Immunofluorescence staining of sections from frozen nodules followed by microscopical analysis was performed to investigate whether ETs were encapsulating

nodules or in localized in the lymphocystis nodules. The analysis showed that web-like extracellular DNA fibers labeled by DAPI were co-localized with citrullinated histone H3 (CitH3), labeled by Alexa Fluor® 649 goat anti-mouse IgG, in the periphery of the lymphocystis nucleus (Figure 3). The ET-associated DNA were mostly wrapped around the nodule cells and seemed to keep the cells close to each other with full or partial occlusion of the gap junctions.

3.4 | LCDV-induced release of ETs from peritoneal cells

To ascertain whether LCDV induces any formation of ETs, peritoneal cells of healthy black rockfish were isolated and incubated with LCDV for 4 hours. A classical fibrous ET structure protruding extracellularly from peritoneal cells was observed by fluorescence microscopy, indicating the ability of peritoneal cells to release ETs following LCDV stimulus/infection (Figure 4a). LCDV-positive signals were observed on the surface of peritoneal cells, revealing that LCDV could attach to, infect or be phagocyted by peritoneal cells. Moreover, LCDV virions were clearly co-localized in the web-like networks of extracellular DNA (Figure 4a). No specific fluorescence was observed in the control cells.

Since LCDV induced apparent formation of ETs from peritoneal cells it was pertinent to quantify the ET. The quantitation of ETs released from cells was measured by a fluorescence spectrophotometer. The ET-formation of PMA- and LCDV stimulated cells were significantly higher than from control cells at all time points. The ET-formation from the LCDV-stimulated cells were significantly higher compared to the PMA-stimulated group at the corresponding time points (P <0.05). In the PMA- and

LCDV-stimulated groups, the ETs release increased significantly from 1 to the 4 hr (Figure 4b).

4 | DISCUSSION

~~When fish are infected by LCDV, lymphocystis cells are formed (Colorni & Diamant, 1995; Sarasquete et al., 1998).~~ LCDV preferentially infects fibroblastic cells in the connective tissue of dermis. The virus infection causes to hypertrophy of fibroblasts and cease mitosis, resulting in the formation of spherical mast cells (Paperna et al., 1982). At the same time, the nuclei of the cells undergo degenerative changes, such as pyknosis and karyorrhexis, while basophilic inclusions of varying sizes are scattered at the cytoplasmic margins (Muthuramalingam, 2014). In our study, the appearance of whitish/greyish/reddish clusters of nodules on the fins and skin as well as hypertrophic LCDV-infected dermal cells, was noted. Hypertrophic cells may reach a diameter of 0.3-2 mm in severe cases (REF). The nuclei of lymphocystis cells were enlarged, irregular and contained basophilic marginated chromatin, with histological characteristics resembling those previously described in different species of fish (REF).

Lymphocystis cells rupture in the later stages of infection where viral particles are released, infecting neighbor tissues and entering the circulatory system, causing systemic infections. Using sensitive immunological and molecular diagnostic methods, LCDV has been detected in different organs of fish without internal lesions, such as the spleen, heart, and gastrointestinal tract (Cano et al., 2006, 2007). Fibroblasts, hepatocytes and macrophages appear to be target cells for virus replication (Cano et al.,

2009). In this study, an immunocytochemical study was performed to confirm that peritoneal cells can be directly infected by LCDV *in vitro*. In teleost fish, resident peritoneal cavity cells contain different immune cells such as lymphocytes, granulocytes, macrophages, dendritic cells which have ability to function during inflammatory response, antigen presentation, and clearance of pathogens (Shi et al., 2022). In other studies, different type of immune cells have been shown to be involved in the defense against LCDV disease. The proliferation of macrophages and epithelioid cells around lymphocystis cells has been previously described as an immune response to LCDV in *Pleuronectes platessa* (Roberts, 1976), *Sciaenops ocellatus* (Colorni & Diamant, 1995) and *Sebastes schlegeli* (Sheng et al., 2007). Dezfuli et al. (2012) demonstrated that piscidin 3-expressing acidophilic granulocytes are recruited and activated in the dermis of gilthead sea bream in response to LCDV infection. In addition, increased phagocytic capability was observed in head kidney cells from American plaice suffering from LCD, where most of them were neutrophils and macrophages which potentiality are able to release ETs (Marcogliese et al., 2001). In our histopathological study, we discovered that a substantial number of inflammatory cells were localized in the area around the lymphocystis cells, where some released ETs, suggesting that these cells might perform a function in regulating the inflammatory response against LCDV infection. Moreover, ETs was observed on the surface of fish lymphocystis nodules as well as in mucus. Significantly higher quantity of ETs was covering large nodules compared to smaller ones. These findings suggested that ETs may be important during immunological responses that follows infection with LCDV

284 infection.

285 Studies both *in vitro* and *in vivo* have demonstrated that the sticky, web-like
286 structure of ETs can bind and sequester virions, preventing them from reaching their
287 target cells and express antiviral factors, such as myeloperoxidase and β-defensin.
288 Moreover, ETs have been shown to directly inhibit virus replication and protein
289 synthesis (Hao et al., 2021; Saitoh et al., 2012). Our study confirmed that the peritoneal
290 cells ETs caught LCDV virions *in vitro*. Quantitative analysis revealed that ETs
291 production was dependent on the inoculation time. As such, the formation of ETs may
292 be an important mechanism of a local anti-LCDV response to limit viral spread
293 (Nakazawa et al., 2018).

294 Despite the beneficial effects of ETs in controlling pathogens, sustained
295 formations of ETs during respiratory viral infections are associated with a collateral
296 tissue injury (Lefrançais et al., 2018). In addition, various studies showed that higher
297 and excessive formations of ETs might activate inflammatory reactions that otherwise
298 induce systemic coagulopathy, localized micro-thrombosis and multiple organ
299 dysfunction syndrome (MOD) (Papayannopoulos, 2018). In mammalian, ETs have
300 been suggested to participate in thrombus growth and stabilization by providing a
301 scaffold for fibrin formation and platelet aggregation (Fuchs et al., 2010). In some
302 affected skin sections, we noticed DNA was wrapped around the cystic cells and seemed
303 to pull inflammatory cells together with full or partial occlusion of the cell junctions,
304 which may play a detrimental role in the elimination of lymphocysts. But, this will
305 require further analysis. In addition, it remains to be determined whether the release of

306 ETs in lymphocysts contributes to viral clearance or, alternatively, if it further promotes
307 skin lesions. Whatever the case is, our data pave the way for future studies aimed at
308 determining the role by granulocytes in the antiviral response of animals.

309 5 | CONCLUSION

310 LCDV is able to induce ETs formation which captured LCDV virions, indicating
311 a central antiviral function of ETs. However, exaggerated ETs formation was observed
312 in the interstitial spaces of the lymphocystis cells which may be beneficial for resolving
313 the inflammation, or it may cause adverse effects such as excessive inflammation.
314

AUTHOR CONTRIBUTIONS

Qian Li, Heng Chi and Roy Ambli Dalmo participated in the conception and design of this study. Qian Li, Xianghu Meng and Heng Chi performed the experimental and statistical analyses. Qian Li and Heng Chi wrote the original draft. Xiaoqian Tang, Xiuzhen Sheng, Jing Xing and Wenbin Zhan revised the manuscript. Roy Ambli Dalmo reviewed and edited the manuscript to the final version. All the authors read and approved this version of the final manuscript.

DATA AVAILABILITY STATEMENT

The original contributions presented in the study are included in the article. Further inquiries can be directed to the corresponding authors.

CONFLICT OF INTEREST STATEMENT

The authors declare that the research was conducted in the absence of any commercial or financial relationships that could be construed as a potential conflict of interest.

REFERENCES

Alfaro, C., Teijeira, A., Oñate, C., Pérez, G., Sanmamed, M. F., Andueza, M. P., Alignani, D., Labiano, S., Azpilikueta, A., Rodriguez-Paulete, A., Garasa, S., Fusco, J. P., Aznar, A., Inogés, S., De Pizzol, M., Allegretti, M., Medina-Echeverz, J., Berraondo, P., Perez-Gracia, J. L., & Melero, I. (2016). Tumor-Produced Interleukin-8 Attracts Human Myeloid-Derived Suppressor Cells and Elicits Extrusion of Neutrophil Extracellular Traps (NETs). *Clinical Cancer Research: An Official Journal of the American Association for Cancer Research*, *22*(15), 3924–3936. https://doi.org/10.1158/1078-0432.CCR-15-2463

Álvarez de Haro, N., Van, A. P., Robb, C. T., Rossi, A. G., & Desbois, A. P. (2021). Release of chromatin extracellular traps by phagocytes of Atlantic salmon, Salmo salar (Linnaeus, 1758). *Fish & Shellfish Immunology*, *119*, 209–219. https://doi.org/10.1016/j.fsi.2021.08.023

Anders, K. (1989). Lymphocystis Disease of Fishes. In W. Ahne & E. Kurstak (Eds.), *Viruses of Lower Vertebrates* (pp. 141–160). Springer. https://doi.org/10.1007/978-3-642-83727-2_14

Azevedo, P. O., Paiva, A. E., Santos, G. S. P., Lousado, L., Andreotti, J. P., Sena, I. F. G., Tagliati, C. A., Mintz, A., & Birbrair, A. (2018). Cross-talk between lung cancer and bones results in neutrophils that promote tumor progression. *Cancer Metastasis Reviews*, *37*(4), 779–790. https://doi.org/10.1007/s10555-018-9759-4

Bertini, R., Allegretti, M., Bizzarri, C., Moriconi, A., Locati, M., Zampella, G., Cervellera, M. N., Di Cioccio, V., Cesta, M. C., Galliera, E., Martinez, F. O., Di Bitondo, R., Troiani, G., Sabbatini, V., D'Anniballe, G., Anacardio, R., Cutrin, J. C., Cavalieri, B., Mainiero, F., … Colotta, F. (2004). Noncompetitive allosteric inhibitors of the inflammatory chemokine

receptors CXCR1 and CXCR2: Prevention of reperfusion injury. *Proceedings of the National Academy of Sciences of the United States of America*, *101*(32), 11791–11796. https://doi.org/10.1073/pnas.0402090101

Cano, I., Alonso, M. C., Garcia-Rosado, E., Saint-Jean, S. R., Castro, D., & Borrego, J. J. (2006). Detection of lymphocystis disease virus (LCDV) in asymptomatic cultured gilt-head seabream (Sparus aurata, L.) using an immunoblot technique. *Veterinary Microbiology*, *113*(1–2), 137–141. https://doi.org/10.1016/j.vetmic.2005.10.038

Cano, I., Ferro, P., Alonso, M. c., Bergmann, S. m., Römer-Oberdörfer, A., Garcia-Rosado, E., Castro, D., & Borrego, J. j. (2007). Development of molecular techniques for detection of lymphocystis disease virus in different marine fish species. *Journal of Applied Microbiology*, *102*(1), 32–40. https://doi.org/10.1111/j.1365-2672.2006.03066.x

Cano, I., Ferro, P., Alonso, M. C., Sarasquete, C., Garcia-Rosado, E., Borrego, J. J., & Castro, D. (2009). Application of in situ detection techniques to determine the systemic condition of lymphocystis disease virus infection in cultured gilt-head seabream, Sparus aurata L. *Journal of Fish Diseases*, *32*(2), 143–150. https://doi.org/10.1111/j.1365-2761.2008.00970.x

Chi, H., & Sun, L. (2016). Neutrophils of Scophthalmus maximus produce extracellular traps that capture bacteria and inhibit bacterial infection. *Developmental and Comparative Immunology*, *56*, 7–12. https://doi.org/10.1016/j.dci.2015.11.005

Colorni, A., & Diamant, A. (1995). Splenic and cardiac lymphocystis in the red drum, Sciaenops ocellatus (L.). *Journal of Fish Diseases*, *18*(5), 467–471. https://doi.org/10.1111/j.1365-2761.1995.tb00339.x

374 Desai, J., Kumar, S. V., Mulay, S. R., Konrad, L., Romoli, S., Schauer, C., Herrmann, M., Bilyy, R.,
375 Müller, S., Popper, B., Nakazawa, D., Weidenbusch, M., Thomasova, D., Krautwald, S.,
376 Linkermann, A., & Anders, H.-J. (2016). PMA and crystal-induced neutrophil extracellular
377 trap formation involves RIPK1-RIPK3-MLKL signaling. *European Journal of Immunology*,
378 *46*(1), 223–229. https://doi.org/10.1002/eji.201545605
379 Dezfuli, B. S., Lui, A., Giari, L., Castaldelli, G., Mulero, V., & Noga, E. J. (2012). Infiltration and
380 activation of acidophilic granulocytes in skin lesions of gilthead seabream, Sparus aurata,
381 naturally infected with lymphocystis disease virus. *Developmental and Comparative*
382 *Immunology*, *36*(1), 174–182. https://doi.org/10.1016/j.dci.2011.06.017
383 Flerova, E. A., & Balabanova, L. V. (2013). [Ultrastructure of granulocytes of bony fishes (orders
384 Salmoniformes, Cypriniformes, Perciformes)]. *Zhurnal Evoliutsionnoi Biokhimii I*
385 *Fiziologii*, *49*(2), 162–171.
386 Fuchs, T. A., Brill, A., Duerschmied, D., Schatzberg, D., Monestier, M., Myers, D. D., Wrobleski,
387 S. K., Wakefield, T. W., Hartwig, J. H., & Wagner, D. D. (2010). Extracellular DNA traps
388 promote thrombosis. *Proceedings of the National Academy of Sciences of the United States*
389 *of America*, *107*(36), 15880–15885. https://doi.org/10.1073/pnas.1005743107
390 Gómez, R. M., López Ortiz, A. O., & Schattner, M. (2021). Platelets and extracellular traps in
391 infections. *Platelets*, *32*(3), 305–313. https://doi.org/10.1080/09537104.2020.1718631
392 González de Canales, M. L., Muñoz-Cueto, J. A., Arellano, J., García-García, A., & Sarasquete, C.
393 (1996). Histological and histochemical characteristics of the lymphocystis disease in
394 gilthead seabream, Sparus aurata L. from the south-atlantic coast of Spain. *European*
395 *Journal of Histochemistry: EJH*, *40*(2), 143–152.

Hao, X., Chi, H., Tang, X., Xing, J., Sheng, X., & Zhan, W. (2021). The Functions of β-Defensin in Flounder (Paralichthys olivaceus): Antibiosis, Chemotaxis and Modulation of Phagocytosis. *Biology*, *10*, 1247. https://doi.org/10.3390/biology10121247

Jenne, C. N., & Kubes, P. (2015). Virus-induced NETs—Critical component of host defense or pathogenic mediator? *PLoS Pathogens*, *11*(1), e1004546. https://doi.org/10.1371/journal.ppat.1004546

Jenne, C. N., Wong, C. H. Y., Zemp, F. J., McDonald, B., Rahman, M. M., Forsyth, P. A., McFadden, G., & Kubes, P. (2013). Neutrophils recruited to sites of infection protect from virus challenge by releasing neutrophil extracellular traps. *Cell Host & Microbe*, *13*(2), 169–180. https://doi.org/10.1016/j.chom.2013.01.005

Katzenback, B. A., & Belosevic, M. (2009). Isolation and functional characterization of neutrophil-like cells, from goldfish (Carassius auratus L.) kidney. *Developmental and Comparative Immunology*, *33*(4), 601–611. https://doi.org/10.1016/j.dci.2008.10.011

Kim, K. H., Hwang, Y. J., & Kwon, S. R. (2001). Influence of daily water temperature changes on the chemiluminescent response and mortality of cultured rockfish (Sebastes schlegeli). *Aquaculture*, *192*(2), 93–99. https://doi.org/10.1016/S0044-8486(00)00460-9

Lefrançais, E., Mallavia, B., Zhuo, H., Calfee, C. S., & Looney, M. R. (2018). Maladaptive role of neutrophil extracellular traps in pathogen-induced lung injury. *JCI Insight*, *3*(3), e98178, 98178. https://doi.org/10.1172/jci.insight.98178

Marcogliese, D. J., Fournier, M., Lacroix, A., & Cyr, D. G. (2001). Non-specific immune response associated with infections of lymphocystis disease virus in American plaice, Hippoglossoides platessoides (Fabricius). *Journal of Fish Diseases*, *24*(2), 121–124.

https://doi.org/10.1046/j.1365-2761.2001.00268.x

Meseguer, J., López-Ruiz, A., & Angeles Esteban, M. (1994). Cytochemical characterization of leucocytes from the seawater teleost, gilthead seabream (Sparus aurata L.). *Histochemistry*, *102*(1), 37–44. https://doi.org/10.1007/BF00271047

Muthuramalingam, U. (2014). Histopathological study of lymphocystis disease virus (LCDV) in cultured false clownfish, Amphiprion ocellaris (Cuvier, 1830) and true clownfish, Amphiprion percula (Lacepede, 1802). *Journal of Coastal Life Medicine*, *2*, 264–269.

Najmeh, S., Cools-Lartigue, J., Rayes, R. F., Gowing, S., Vourtzoumis, P., Bourdeau, F., Giannias, B., Berube, J., Rousseau, S., Ferri, L. E., & Spicer, J. D. (2017). Neutrophil extracellular traps sequester circulating tumor cells via β1-integrin mediated interactions. *International Journal of Cancer*, *140*(10), 2321–2330. https://doi.org/10.1002/ijc.30635

Nakazawa, D., Desai, J., Steiger, S., Müller, S., Devarapu, S. K., Mulay, S. R., Iwakura, T., & Anders, H.-J. (2018). Activated platelets induce MLKL-driven neutrophil necroptosis and release of neutrophil extracellular traps in venous thrombosis. *Cell Death Discovery*, *4*, 6. https://doi.org/10.1038/s41420-018-0073-2

Narasaraju, T., Yang, E., Samy, R. P., Ng, H. H., Poh, W. P., Liew, A.-A., Phoon, M. C., van Rooijen, N., & Chow, V. T. (2011). Excessive neutrophils and neutrophil extracellular traps contribute to acute lung injury of influenza pneumonitis. *The American Journal of Pathology*, *179*(1), 199–210. https://doi.org/10.1016/j.ajpath.2011.03.013

Palić, D., Andreasen, C. B., Ostojić, J., Tell, R. M., & Roth, J. A. (2007). Zebrafish (Danio rerio) whole kidney assays to measure neutrophil extracellular trap release and degranulation of primary granules. *Journal of Immunological Methods*, *319*(1–2), 87–97.

https://doi.org/10.1016/j.jim.2006.11.003

Papayannopoulos, V. (2018). Neutrophil extracellular traps in immunity and disease. *Nature Reviews. Immunology*, *18*(2), 134–147. https://doi.org/10.1038/nri.2017.105

Papayannopoulos, V., Metzler, K. D., Hakkim, A., & Zychlinsky, A. (2010). Neutrophil elastase and myeloperoxidase regulate the formation of neutrophil extracellular traps. *The Journal of Cell Biology*, *191*(3), 677–691. https://doi.org/10.1083/jcb.201006052

Paperna, I., Ilana Sabnai, H., & Colorni, A. (1982). An outbreak of lymphocystis in Sparus aurata L. in the Gulf of Aqaba, Red Sea. *Journal of Fish Diseases*, *5*(5), 433–437. https://doi.org/10.1111/j.1365-2761.1982.tb00500.x

Parker, H., Dragunow, M., Hampton, M. B., Kettle, A. J., & Winterbourn, C. C. (2012). Requirements for NADPH oxidase and myeloperoxidase in neutrophil extracellular trap formation differ depending on the stimulus. *Journal of Leukocyte Biology*, *92*(4), 841–849. https://doi.org/10.1189/jlb.1211601

Pijanowski, L., Golbach, L., Kolaczkowska, E., Scheer, M., Verburg-van Kemenade, B. M. L., & Chadzinska, M. (2013). Carp neutrophilic granulocytes form extracellular traps via ROS-dependent and independent pathways. *Fish & Shellfish Immunology*, *34*(5), 1244–1252. https://doi.org/10.1016/j.fsi.2013.02.010

Raftery, M. J., Lalwani, P., Krautkrämer, E., Peters, T., Scharffetter-Kochanek, K., Krüger, R., Hofmann, J., Seeger, K., Krüger, D. H., & Schönrich, G. (2014). B2 integrin mediates hantavirus-induced release of neutrophil extracellular traps. *The Journal of Experimental Medicine*, *211*(7), 1485–1497. https://doi.org/10.1084/jem.20131092

Rieger, A. M., Konowalchuk, J. D., Grayfer, L., Katzenback, B. A., Havixbeck, J. J., Kiemele, M.

462 D., Belosevic, M., & Barreda, D. R. (2012). Fish and mammalian phagocytes differentially
463 regulate pro-inflammatory and homeostatic responses in vivo. *PloS One*, *7*(10), e47070.
464 https://doi.org/10.1371/journal.pone.0047070
465 Roberts, R. J. (1976). Experimental Pathogenesis of Lymphocystis in the Plaice (Pleuronectes
466 Platessa). In L. A. Page (Ed.), *Wildlife Diseases* (pp. 431–441). Springer US.
467 https://doi.org/10.1007/978-1-4757-1656-6_47
468 Saitoh, T., Komano, J., Saitoh, Y., Misawa, T., Takahama, M., Kozaki, T., Uehata, T., Iwasaki, H.,
469 Omori, H., Yamaoka, S., Yamamoto, N., & Akira, S. (2012). Neutrophil extracellular traps
470 mediate a host defense response to human immunodeficiency virus-1. *Cell Host & Microbe*,
471 *12*(1), 109–116. https://doi.org/10.1016/j.chom.2012.05.015
472 Samalecos, C. P. (1986). Analysis of the structure of fish lymphocystis disease virions from skin
473 tumours of pleuronectes. *Archives of Virology*, *91*(1–2), 1–10.
474 https://doi.org/10.1007/BF01316723
475 Sarasquete, C., González de Canales, M. L., Arellano, J., Pérez-Prieto, S., García-Rosado, E., &
476 Borrego, J. J. (1998). Histochemical study of lymphocystis disease in skin of gilthead
477 seabream, Sparus aurata L. *Histology and Histopathology*, *13*(1), 37–45.
478 https://doi.org/10.14670/HH-13.37
479 Schauer, C., Janko, C., Munoz, L. E., Zhao, Y., Kienhöfer, D., Frey, B., Lell, M., Manger, B., Rech,
480 J., Naschberger, E., Holmdahl, R., Krenn, V., Harrer, T., Jeremic, I., Bilyy, R., Schett, G.,
481 Hoffmann, M., & Herrmann, M. (2014). Aggregated neutrophil extracellular traps limit
482 inflammation by degrading cytokines and chemokines. *Nature Medicine*, *20*(5), 511–517.
483 https://doi.org/10.1038/nm.3547

484 Sheng, X., Zhan, W., Xu, S., & Cheng, S. (2007). Histopathological observation of lymphocystis
485 disease and lymphocystis disease virus (LCDV) detection in cultured diseased Sebastes
486 schlegeli. *Journal of Ocean University of China*, *6*(4), 378–382.
487 https://doi.org/10.1007/s11802-007-0378-x
488 Shi, X., Chi, H., Sun, Y., Tang, X., Xing, J., Sheng, X., & Zhan, W. (2022). The Early Peritoneal
489 Cavity Immune Response to Vibrio Anguillarum Infection and to Inactivated Bacterium in
490 Olive Flounder (Paralichthys olivaceus). *Microorganisms*, *10*(11), 2175.
491 https://doi.org/10.3390/microorganisms10112175
492 Teijeira, Á., Garasa, S., Gato, M., Alfaro, C., Migueliz, I., Cirella, A., de Andrea, C., Ochoa, M. C.,
493 Otano, I., Etxeberria, I., Andueza, M. P., Nieto, C. P., Resano, L., Azpilikueta, A., Allegretti,
494 M., de Pizzol, M., Ponz-Sarvisé, M., Rouzaut, A., Sanmamed, M. F., … Melero, I. (2020).
495 CXCR1 and CXCR2 Chemokine Receptor Agonists Produced by Tumors Induce
496 Neutrophil Extracellular Traps that Interfere with Immune Cytotoxicity. *Immunity*, *52*(5),
497 856-871.e8. https://doi.org/10.1016/j.immuni.2020.03.001
498 Urban, C. F., Ermert, D., Schmid, M., Abu-Abed, U., Goosmann, C., Nacken, W., Brinkmann, V.,
499 Jungblut, P. R., & Zychlinsky, A. (2009). Neutrophil extracellular traps contain calprotectin,
500 a cytosolic protein complex involved in host defense against Candida albicans. *PLoS*
501 *Pathogens*, *5*(10), e1000639. https://doi.org/10.1371/journal.ppat.1000639
502 Wang, M., Sheng, X.-Z., Xing, J., Tang, X.-Q., & Zhan, W.-B. (2011). Identification of a 27.8 kDa
503 protein from flounder gill cells involved in lymphocystis disease virus binding and
504 infection. *Diseases of Aquatic Organisms*, *94*(1), 9–16. https://doi.org/10.3354/dao02311
505 Warnatsch, A., Ioannou, M., Wang, Q., & Papayannopoulos, V. (2015). Inflammation. Neutrophil

extracellular traps license macrophages for cytokine production in atherosclerosis. *Science (New York, N.Y.)*, *349*(6245), 316–320. https://doi.org/10.1126/science.aaa8064

Weiß, E., & Kretschmer, D. (2018). Formyl-Peptide Receptors in Infection, Inflammation, and Cancer. *Trends in Immunology*, *39*(10), 815–829. https://doi.org/10.1016/j.it.2018.08.005

Wen, L.-L., Zhao, M.-L., Chi, H., & Sun, L. (2018). Histones and chymotrypsin-like elastases play significant roles in the antimicrobial activity of tongue sole neutrophil extracellular traps. *Fish & Shellfish Immunology*, *72*, 470–476. https://doi.org/10.1016/j.fsi.2017.11.004

Wilhelm Filho, D. (2007). Reactive oxygen species, antioxidants and fish mitochondria. *Frontiers in Bioscience: A Journal and Virtual Library*, *12*, 1229–1237. https://doi.org/10.2741/2141

Zhan, W., Li, Y., Sheng, X., Xing, J., & Tang, X. (2010). Detection of lymphocystis disease virus in Japanese flounder Paralichthys olivaceus and other marine teleosts from northern China. *Chinese Journal of Oceanology and Limnology*, *28*(6), 1213–1220. https://doi.org/10.1007/s00343-010-9934-0

Zhong, Y., Tang, X., Sheng, X., Xing, J., & Zhan, W. (2018). Development and Characterization of Monoclonal Antibodies to the 32 kDa Viral Attachment Protein of Lymphocystis Disease Virus and Their Neutralizing Ability in Vitro. *International Journal of Molecular Sciences*, *19*(9), 2536. https://doi.org/10.3390/ijms19092536

Figure legends:

FIGURE 1 Macroscopic and microscopic view of LDCV-infected black rockfish. (a) Lymphocystis disease virus infected black rockfish, the nodules on fins and body surface being shown by arrows. (b-c) Histological section images of lymphocystis disease (LCD) lesion samples. (c) is zoom of the boxed regions in (b). Abundant basophilic fibrillar filaments accumulate at the periphery of the hypertrophic lymphocystis cells showed by arrows without tail. Scale bar = 100 μm.

FIGURE 2 Representative macrophotographs of LCDV-infected black rockfish and microscopic view of ETs on the surface of nodules. (a-c) Fluorescent microphotographs showing extracellular DNA aggregates stained with Sytox green on the surface of nodules. (a) The surface of the nodule under light microscope observation. (b) The extracellular DNA aggregates and nuclei in dead cells stained with Sytox green on the surface of the same field of (b) under fluorescence microscope observation. (c) Merge of the picture (a) and (b). Scale bars = 40 μm. (d-e) *In vivo* imaging of nodules on the fins, previously immersed in an aqueous Sytox Green solution, under oblique white light (d) and 488 nm light (e) illumination, respectively. The fluorescence intensity indicates the quantity of the extracellular DNA dyed by Sytox Green. (f) SEM analysis of the ETs release from mucus scraped from the surface of the nodules. Scale bars = 50 μm.

FIGURE 3 Presence of abundant ETs in Lymphocystis nodules samples obtained from a black rockfish. Frozen section of nodules stained for CitHistion H3 (red) and DNA (blue) and analyzed using a fluorescence microscope. The expelled DNA colocalized

with CitHistion H3 spread outside cells. Scale bar = 20 μ m

FIGURE 4 LCDV trigger ET-formation of peritoneal cells *in vitro*. (a) Fluorescence microscopy of peritoneal cells after incubation with PBS (control) and LCDV at 4 hours. Co-localization of expelled DNA (blue) with the LCDV (red) was observed. Viral capture (co-localization) by the extracellular DNA networks is observed under LCDV stimulated (arrow). Scale bars = 10 μm. (b) Time course production of ETs by peritoneal cells after stimulation with PBS, PMA or LCDV for different times. The results represented three independent experiments. Different letters above the bar represent the statistical significance ($P < 0.05$). Error bars represent standard errors of SD.

Figure 1

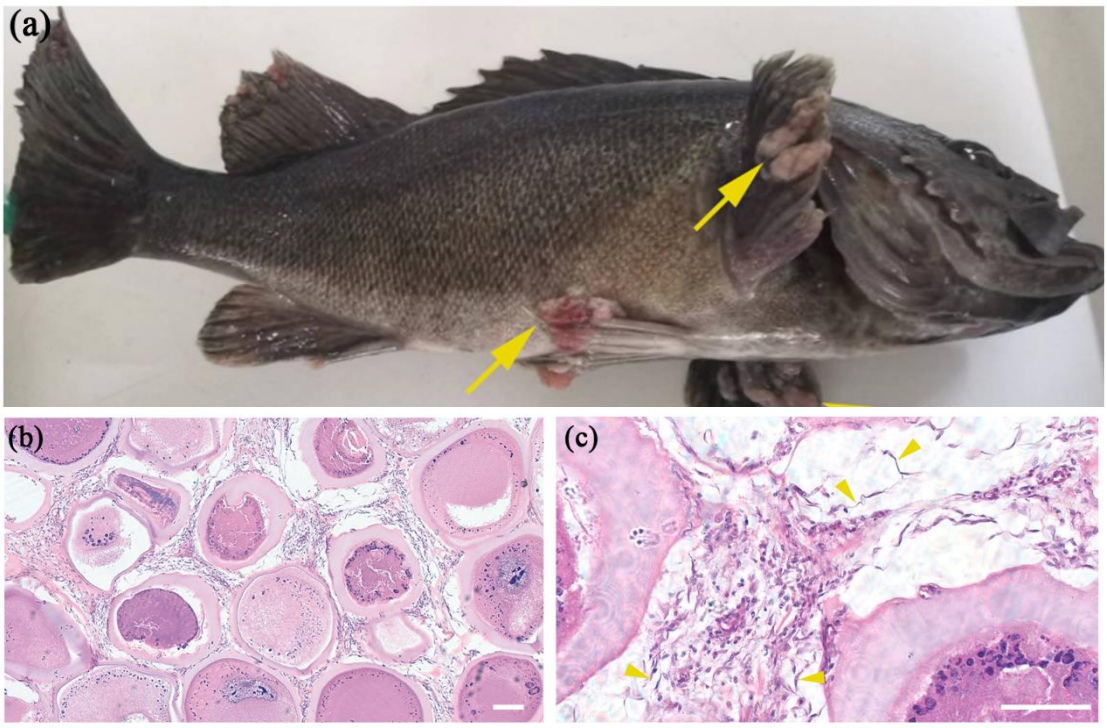

572 **Figure 2**

573 574 575 576 577 578

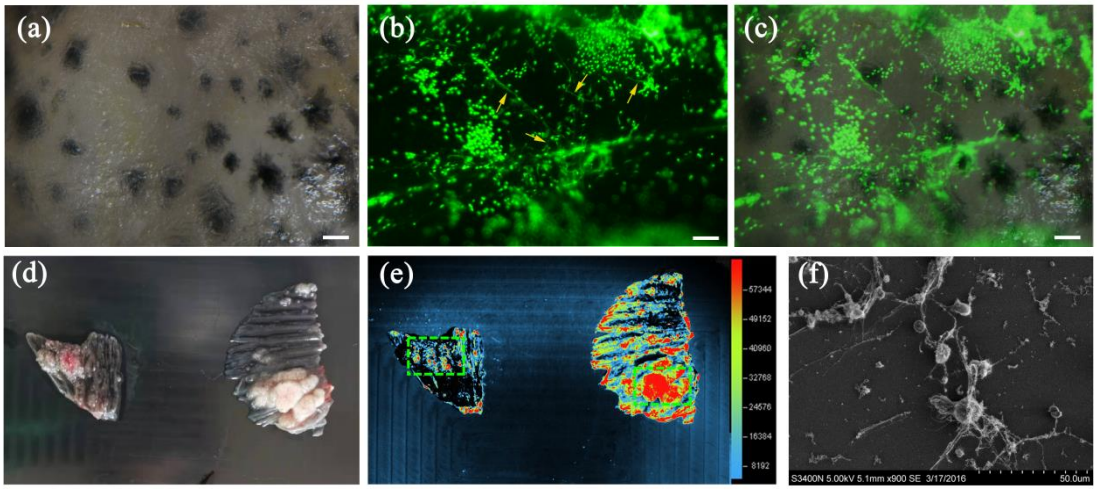

579

580

581

582

583 **Figure 3**

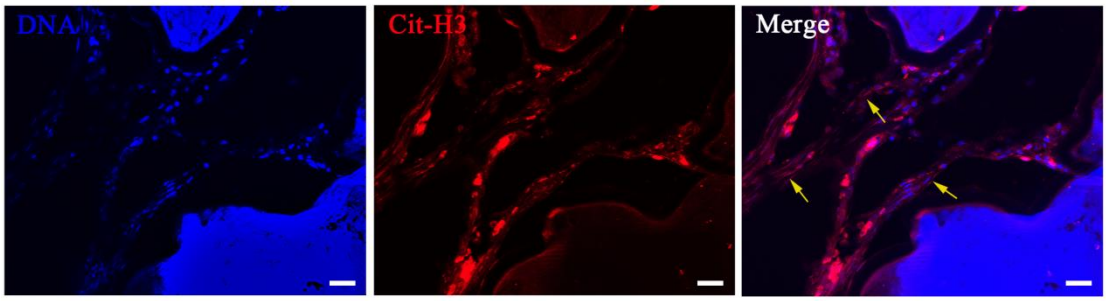

584

585

586

587

588

589

590

591

592

593

Figure 4

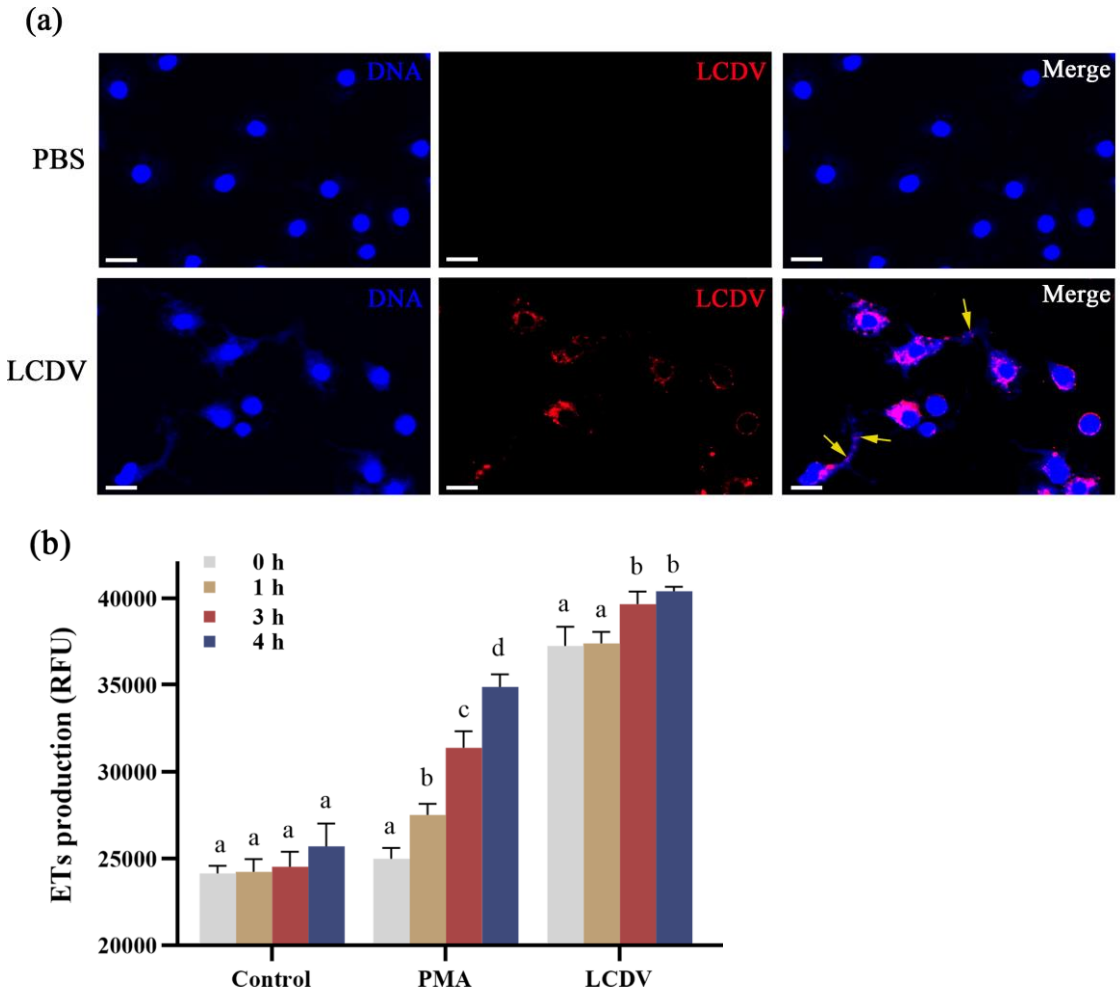
(a)
PBS
LCDV
DNA
LCDV
Merge
DNA
LCDV
Merge
(b)
0 h
1 h
3 h
4 h
ETs production (RFU)
40000
35000
30000
25000
20000
a a a a
a b c d
a a b b
Control
PMA
LCDV